Eur. Phys. J. C 25, 553–561 (2002)
Digital Object Identifier (DOI) 10.1140/epjc/s2002-01030-5

THE EUROPEAN PHYSICAL JOURNAL C

QED box amplitude in heavy fermion production

J. Portolés, P.D. Ruiz-Femenía

Departament de Física Teòrica, IFIC, Universitat de València – CSIC, Apt. Correus 22085, 46071 València, Spain

Received: 13 June 2002 /
Published online: 24 September 2002 –

Abstract. We evaluate the two-photon box contribution to heavy fermion production in electron positron annihilation, that provides $\mathcal{O}(\alpha^2)$ electromagnetic corrections to the Born cross section. The study of its non-relativistic expansion, relevant at energies close to the threshold of production, is also performed. We also verify that the threshold expansion of the one-loop integrals correctly reproduces our results, thus extending the applicability of this technique to heavy fermion production diagrams.

1 Introduction

Heavy fermion production processes out of electron positron annihilation, $e^+e^- \to f\bar{f}$, have become a subject of thorough study in the last years. Their interest embodies multiple features and a wide energy range, from close to threshold production to high-energy colliders. LEP and LEP2 have provided the appropriate tool pushing behind this burst. In addition this is among the scattering processes with a higher expected number of events at a future Linear Collider running in the 0.5 TeV–1 TeV energy region like TESLA and NLC/JLC-X, or CLIC at higher energies. Their interest arises mainly from the possibility of exploring new physics and, therefore, an accurate description within the standard model is necessary for the analyses of data. Projects like ZFITTER [1] and the ongoing CalcPHEP [2,3] aim to provide the relevant theoretical framework for that purpose.

QED corrections seem to be of little interest when probing the quantum effects within the standard model, but it is obvious that their contribution, however small, should be considered in order to disentangle new physics effects. Besides, if a deeper understanding of the physical parameters of heavy fermions is intended, electromagnetic $\tau^+\tau^-$ and heavy quark $Q\overline{Q}$ production out of e^+e^- annihilation at threshold energies supplies the required information.

From a theoretical point of view $e^+e^- \to f\bar{f}$ cross sections close to threshold evaluated within perturbation theory are misleading due to the presence, in the physical system, of a kinematical variable of the same order as the gauge theory coupling: the velocity of the heavy fermion pair in the center of mass of the colliding system, $\beta = (1 - 4M^2/s)^{1/2}$, with M the mass of the f fermion. Hence, when $\beta \sim \alpha$, care has to be taken in order to resum terms as $(\alpha/\beta)^n$ or $(\alpha \ln \beta)^n$ that can give potentially large contributions [4]. Recently the development of non-relativistic effective field theories of QED and QCD [5] enabled one to implement the suitable systematic procedure to follow. Facilities as the proposed Tau-Charm Factory, a high-luminosity e^+e^- collider with a center-of-mass energy near the $\tau^+\tau^-$ production threshold [6], would provide excellent information on the mass of this lepton [7]. Moreover an accurate determination of the mass of the top quark (difficult to get at the next hadron colliders) requires a future lepton collider at the $t\bar{t}$ threshold [8]. Consequently a thorough study of the non-relativistic contribution to $\sigma(e^+e^- \to f\bar{f})$ both from electromagnetic and strong interactions is mandatory.

In [7] a detailed study of the threshold behavior of $\sigma(e^+e^- \to \tau^+\tau^-)$ was performed, and it was pointed out that, within the $\mathcal{O}(\alpha^2)$ electromagnetic corrections to the Born cross section, the squared amplitude of the box diagram involving two-photon $\tau^+\tau^-$ production (see Fig. 1) had not been considered yet. The electroweak one-loop contributions to the $e^+e^- \to f\bar{f}$ process were evaluated in [9]. Here this box contribution was already taken into account, though an explicit expression was only given for the $M = 0$ case. In this paper we provide the amplitude of this diagram for a final massive fermion[1].

Once the explicit result is worked out we perform its non-relativistic expansion in terms of the velocity β and we find that the contribution of this diagram to the cross section is of $\mathcal{O}(\alpha^4\beta^3)$, that is, $\mathcal{O}(\alpha^2\beta^2)$ over the Born cross section. The additional suppression driven by the velocity squared indicates that the contribution of the two-photon box diagram to the production of heavy fermions at threshold is negligible compared to the precision foreseen in the next future.

In Sect. 2 we give details on the calculation of the box diagram contributing to $e^+e^- \to f\bar{f}$ in the limit when $m_e \ll M$, and we provide the full analytical result. Section 3 is dedicated to the study of the threshold behavior

[1] While writing this article [3] appeared. In this preprint a full expression for the QED box diagram amplitude is also given

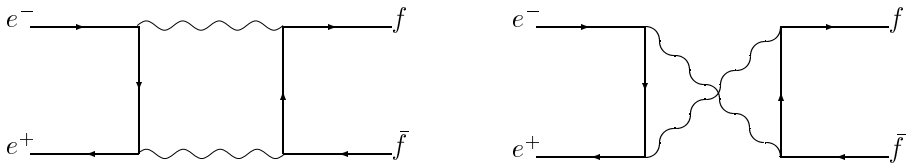

Fig. 1a,b. Direct **a** and crossed **b** box diagrams for $e^+e^- \to f\bar{f}$

of the box amplitude as obtained directly from our previous result. We confirm the features of this threshold amplitude by performing an alternative analysis of the integrals through the asymptotic expansion method in Sect. 4. Our conclusions are collected in Sect. 5. Finally, two appendices contain the basic scalar integrals appearing in this article and a comment on the infrared divergent part of the box amplitude.

2 Two-photon box diagram

The contribution to the S-matrix of the process $e^-(p)$ $e^+(p') \to f(k)\bar{f}(k')$ of the two-photon box amplitudes is depicted in Fig. 1 and it is defined by

$$\langle f\bar{f}|\mathrm{i}\mathcal{T}|e^+e^-\rangle_{\mathrm{box}} = (2\pi)^4\delta(p+p'-k-k')\mathrm{i}\mathcal{M}_{\mathrm{box}}. \quad (1)$$

As we are interested in heavy fermion production we will perform the evaluation for $k^2 = k'^2 = M^2$ and $p^2 = p'^2 = m^2 \ll M^2$ (we neglect the electron mass where possible). The two-photon box amplitude is gauge invariant and, consequently, we perform the calculation by taking the Feynman choice. The direct box amplitude, Fig. 1a, is written down following QED Feynman rules as follows:

$$\mathcal{M}_a = e^4Q_f^2\int\frac{\mathrm{d}^4\ell}{\mathrm{i}(2\pi)^4}\times \quad (2)$$
$$\frac{\{\bar{v}_e(p')\gamma^\mu\not{\ell}\gamma^\nu u_e(p)\}\{\bar{u}_f(k)\gamma_\nu(\not{k}-\not{p}+\not{\ell}+M)\gamma_\mu v_f(k')\}}{(\ell^2-m^2)[(\ell+k-p)^2-M^2][(\ell-p)^2-\lambda^2][(\ell+p')^2-\lambda^2]},$$

where we have introduced a photon mass λ in order to regularize the infrared divergences known to be present in this amplitude. The crossed box diagram in Fig. 1b can be obtained from (2) by adding an overall minus sign, reversing the order of the γ_μ, γ_ν matrices in the heavy fermion bilinear, and performing the substitutions $k \to k'$ everywhere (except for the spinors) and $M \to -M$. Hence, in (1), $\mathcal{M}_{\mathrm{box}} = \mathcal{M}_a + \mathcal{M}_b$. The evaluation of the integrals is slightly cumbersome but straightforward, and the details are given in Appendix A.

With the definition of the Mandelstam variables $s = (p+p')^2$ and $t = (p-k)^2$, the spinor structure of $\mathcal{M}_{\mathrm{box}}$ is decomposed into four sets of amplitudes $L_i^{\rho\kappa}$ multiplied by the corresponding coefficients w_i^ρ:

$$\mathcal{M}_{\mathrm{box}}(\kappa;s,t) = e^4Q_f^2\sum_{i=1}^{4}\sum_{\rho=\pm1}L_i^{\rho\kappa}w_i^\rho, \quad (3)$$

with the basic amplitudes

$$L_1^{\rho\kappa} = [\bar{v}_e(p')\gamma_\mu P_\kappa u_e(p)][\bar{u}_f(k)\gamma^\mu(1+\kappa\rho\gamma_5)v_f(k')],$$
$$L_2^{\rho\kappa} = [\bar{v}_e(p')\not{k}P_\kappa u_e(p)][\bar{u}_f(k)\not{p}(1+\kappa\rho\gamma_5)v_f(k')],$$
$$L_3^{\rho\kappa} = [\bar{v}_e(p')\not{k}P_\kappa u_e(p)][\bar{u}_f(k)(1+\kappa\rho\gamma_5)v_f(k')],$$
$$L_4^{\rho\kappa} = [\bar{v}_e(p')\gamma_\mu P_\kappa u_e(p)][\bar{u}_f(k)\gamma^\mu\not{p}(1+\kappa\rho\gamma_5)v_f(k')]. \quad (4)$$

The latter have been written in terms of the initial state e^+e^- chiral projectors

$$P_\kappa = \frac{1}{2}(1+\kappa\gamma_5), \quad \kappa = \pm1, \quad (5)$$

which, as we are considering massless initial fermions, satisfy $P_\kappa u_e(p) = u_e(p)$, κ being the initial electron helicity; in the massless limit, the positron helicity is forced to be $-\kappa$ in order to have a non-vanishing amplitude. The dependence of $\mathcal{M}_{\mathrm{box}}$ on the spin state of the final state fermions has not been explicitly stated.

The w_i^ρ coefficients can be written in terms of four auxiliary functions $\mathcal{F}_i$, $i = 0,1,2,3$:

$$\begin{aligned}
w_1^+ &= \frac{1}{2}\mathcal{F}_0(s,t),\\
w_1^- &= -\frac{1}{2}\mathcal{F}_0(s,u),\\
w_2^+ &= \mathcal{F}_1(s,t)+\mathcal{F}_2(s,t),\\
w_2^- &= \mathcal{F}_1(s,u)+\mathcal{F}_2(s,u),\\
w_3^+ &= M(\mathcal{F}_1(s,u)-\mathcal{F}_1(s,t)+\mathcal{F}_3(s,u)-\mathcal{F}_3(s,t)),\\
w_3^- &= M(\mathcal{F}_3(s,u)-\mathcal{F}_3(s,t)),\\
w_4^+ &= -\frac{1}{2}M(\mathcal{F}_2(s,t)-\mathcal{F}_2(s,u)),\\
w_4^- &= \frac{1}{2}M(\mathcal{F}_2(s,t)-\mathcal{F}_2(s,u)),
\end{aligned} \quad (6)$$

that read

$$\begin{aligned}
\mathcal{F}_0(s,t) &= \mathcal{F}_0^\lambda(s,t)+\frac{M^2-t}{(M^2-t)^2+st}\\
&\times\left\{t\,(sD_0-2C_t)-M^2\frac{M^2-s-t}{M^2-t}\left(s\overline{D}_0-2\overline{C}_t\right)\right.\\
&\left.-\left(2M^2-s-2t\right)(C_s+C_M)\right\},
\end{aligned} \quad (7)$$

$$\begin{aligned}
\mathcal{F}_1(s,t) &= \frac{1}{(M^2-t)^2+st}\\
&\times\left\{2(B_t-B_s)+\frac{4M^2}{M^2-t}(B_M-B_t)+\frac{M^2-t}{(M^2-t)^2+st}\right.\\
&\times\left[(2M^2-s-2t)\left((M^2-t)(sD_0-2C_t)+sC_s\right)\right.\\
&\left.\left.+\left(2(M^2-t)^2+s(2t+s-4M^2)\right)C_M\right]\right\},
\end{aligned} \quad (8)$$

$$\mathcal{F}_2(s,t) = \mathcal{F}_2^{\lambda}(s,t) - \frac{1}{(M^2-t)^2+st} \times \Big\{(M^2+t)\,(sD_0-2C_t) - (s-4M^2)C_M - (2M^2-s-2t)C_s\Big\}, \quad (9)$$

$$\mathcal{F}_3(s,t) = \frac{1}{(M^2-t)^2+st} \times \left\{ \frac{2t}{M^2-t}(B_t-B_M) + \frac{2(M^2+t)}{4M^2-s}(B_s-B_M) - \frac{(M^2-t)^2}{(M^2-t)^2+st}[(M^2-t)(sD_0-2C_t)+sC_s] + \frac{1}{(4M^2-s)((M^2-t)^2+st)} \times \Big[-4M^8+6(s+2t)M^6-(s+2t)(s+6t)M^4 + 2t(s^2+ts+2t^2)M^2+s^2t^2\Big]C_M \right\}. \quad (10)$$

Full expressions for the scalar functions B_s, B_t, B_M, C_s, C_t, $\overline{C}_t$, C_M, D_0 and $\overline{D}_0$ can be found in (A.5)–(A.13) of Appendix A. It can be seen from $\mathcal{F}_1(s,t)$ and $\mathcal{F}_3(s,t)$ that the two-point functions B_t, B_s and B_M only appear in non-divergent combinations, while the rest of scalar integrals in $\mathcal{F}_i(s,t)$ are UV finite. Clearly $\mathcal{M}_{\rm box}(\kappa;s,t)$ is ultraviolet finite. Scalar integrals D_0 ($\overline{D}_0$) and C_t ($\overline{C}_t$) are infrared divergent for vanishing photon mass λ; however, the combinations sD_0–$2C_t$ and $s\overline{D}_0$–$2\overline{C}_t$ are divergenceless. Hence all the divergences in the $\mathcal{F}_i(s,t)$ functions are collected in $\mathcal{F}_0^{\lambda}(s,t)$ and $\mathcal{F}_2^{\lambda}(s,t)$, given by

$$\mathcal{F}_0^{\lambda}(s,t) = 2\left(M^2-s-t\right)\overline{D}_0, \qquad \mathcal{F}_2^{\lambda}(s,t) = 2D_0, \quad (11)$$

and we get for the infrared divergent part of the box amplitude

$$\mathcal{M}_{\rm box}^{\rm IR} = \frac{e^4Q_f^2}{8\pi^2 s}\left(L_1^{+\kappa}+L_1^{-\kappa}\right)\ln\left(\frac{M^2-u}{M^2-t}\right)\ln\left(\frac{-s-{\rm i}\delta}{\lambda^2}\right). \quad (12)$$

A more complete discussion on the infrared structure of the QED box diagram and the determination of $\mathcal{M}_{\rm box}^{\rm IR}$ is relegated to Appendix B.

Incidentally our result can be used to evaluate a similar two-gluon box contribution to the heavy quark production out of light quarks, $q(A)\bar{q}(B) \to Q(C)\overline{Q}(D)$ (between parentheses we label the color quantum numbers). In order to get this amplitude we need to substitute the $e^4Q_f^2$ factor in (3) by $g_s^4(t^bt^a)_{BA}\{t^a,t^b\}_{CD}$ (a sum over repeated indices is implied)[2].

We have checked that our amplitude in (3), when summed over the polarizations, coincides with a recent result found in [3], though these authors use a different basis of spinor operators. Moreover, from our calculation for $\mathcal{M}_{\rm box}$, we can recover the case where the final fermions are massless. The limit $M \to 0$ can be directly applied to the $w_i^{\pm}$ coefficients, (6), and to the scalar integrals quoted in Appendix A. Within this limit our result agrees with the earlier calculation in [9].

3 Heavy fermion production at threshold

Close to $f\bar{f}$ threshold, it is more convenient to expand the production amplitude in terms of the fermions velocity in the center of mass of the colliding system $\beta = (1-4M^2/s)^{1/2}$. Hence production amplitudes are written in a combined expansion in powers of α and β, and the importance of each contribution is estimated taking $\alpha \sim \beta$. This feature spoils the perturbative expansion in QED due to the appearance of $\mathcal{O}(\alpha^n/\beta^n)$ and $\mathcal{O}(\alpha^m \ln^n \beta)$ terms that diverge as $\beta \to 0$. As a consequence, a resummation of such terms is necessary to avoid a breakdown of the perturbative series, and well-known results from the familiar non-relativistic quantum mechanics are obtained. Nevertheless it is somewhat misleading to associate the appearance of these Coulomb terms to the non-relativistic motion of the fermion pair, as the scattering amplitude calculated from quantum mechanics does not show any kinematic singularity close to threshold: their ultimate origin is the inadequacy of the diagrammatic QED expansion in powers of α to account for the correct non-relativistic dynamics. Keeping this in mind, one should not discard, a priori, divergent terms in the velocity appearing in any QED diagram involving fermions with small velocities.

In [7] it was pointed out that the contribution at threshold of the two-photon box diagram should be analyzed in a NNLO calculation of $\sigma(e^+e^- \to \tau^+\tau^-)$. In this section we proceed to perform the expansion on $\mathcal{M}_{\rm box}$ as given in (3). The leading terms in the velocity expansion of the coefficients $w_i^{\pm}$ can be obtained by taking into account the dependence of the Mandelstam invariants s,t,u on the velocity β and the angle θ between the momenta of the heavy fermion and the electron in the colliding center-of-mass system. The relation is given by

$$s = \frac{4M^2}{1-\beta^2}, \quad t = M^2 - \frac{2M^2}{1-\beta^2}(1-\beta\cos\theta), \quad u = M^2 - \frac{2M^2}{1-\beta^2}(1+\beta\cos\theta). \quad (13)$$

Carrying these expressions to the $w_i^{\pm}$ coefficients displayed in (6) and neglecting $\mathcal{O}(\beta^2)$ terms we obtain

$$w_1^+ = \frac{1}{384M^2\pi^2}\left[-\pi^2+3\ln^2\frac{4M^2}{\lambda^2}-3\ln^2\frac{m^2}{\lambda^2} + \left(8-14{\rm i}\pi-8\ln 2+12\ln\frac{4M^2}{\lambda^2}\right)\beta\cos\theta\right]+\mathcal{O}(\beta^2),$$

$$w_1^- = -w_1^+(\beta\to-\beta),$$

$$w_2^+ = \frac{1}{384M^4\pi^2}$$

[2] In this color factor $t^i = \lambda^i/2$, where λ^i are the $SU(3)$ Gell-Mann matrices and ${\rm Tr}(t^it^j) = \delta^{ij}/2$

$$
\begin{aligned}
&\times \left[\pi^2 - 8 + 8\mathrm{i}\pi + 8\ln 2 - 3\ln^2\frac{4M^2}{\lambda^2} + 3\ln^2\frac{m^2}{\lambda^2}\right.\\
&+ \left(\pi^2 - 34 + 4\mathrm{i}\pi + 16\ln 2 + 12\ln\frac{4M^2}{\lambda^2}\right.\\
&\left.\left. - \; 3\ln^2\frac{4M^2}{\lambda^2} + 3\ln^2\frac{m^2}{\lambda^2}\right)\beta\cos\theta\right] + \mathcal{O}(\beta^2),\\
w_2^- &= w_2^+(\beta\to-\beta),\\
w_3^+ &= \frac{1}{240M^3\pi^2}(37 + 2\mathrm{i}\pi - 64\ln 2)\beta\cos\theta + \mathcal{O}(\beta^2),\\
w_3^- &= \frac{-1}{480M^3\pi^2}(11 + \mathrm{i}\pi - 32\ln 2)\beta\cos\theta + \mathcal{O}(\beta^2),\\
w_4^+ &= \frac{-1}{384M^3\pi^2}\\
&\times \left(\pi^2 + 6\mathrm{i}\pi - 48\ln 2 + 12\ln\frac{4M^2}{\lambda^2} - 3\ln^2\frac{4M^2}{\lambda^2}\right.\\
&\left. + \; 3\ln^2\frac{m^2}{\lambda^2}\right)\beta\cos\theta + \mathcal{O}(\beta^2),\\
w_4^- &= -w_4^+. \qquad (14)
\end{aligned}
$$

The amplitudes $L_i^{\rho\kappa}$, containing fermion wave functions, must also be expanded in terms of β to fulfill the expansion of $\mathcal{M}_{\rm box}$ at small velocities. We shall not give the full result of such an expansion, but just quote their leading behavior, which can easily be obtained by choosing an explicit representation of the gamma matrices and spinors. We thus get

$$
L_1^{\rho\kappa} = \mathcal{O}(1),\; L_2^{\rho\kappa} = \mathcal{O}(\beta),\; L_3^{\rho\kappa} = \mathcal{O}(\beta),\; L_4^{\rho\kappa} = \mathcal{O}(1). \qquad (15)
$$

The terms quoted in (14) together with the expansion in (15) allow us to obtain the leading near threshold contribution to the cross section of the box amplitude $\mathcal{M}_{\rm box}$. Recall that, by virtue of Furry's theorem, the interference of the QED box amplitude with other one-loop amplitudes for the process $e^+e^-\to f\bar f$ vanishes and, consequently, $|\mathcal{M}_{\rm box}|^2$ adds incoherently to the rest of $\mathcal{O}(\alpha^4)$ corrections to $\sigma(e^+e^-\to f\bar f)$, as studied in [7]. The final result for the squared and averaged box amplitude is

$$
\begin{aligned}
\frac{1}{4}\sum_{\rm pol.}|\mathcal{M}_{\rm box}|^2 &= (Q_f\alpha)^4\left\{\frac{16}{9}(\pi^2 + (1-\ln 2)^2)\right. \qquad (16)\\
&+ \left[-\frac{1}{2}L_M^4 - 4L_M^3 - 2L_M^3\ell_m\right.\\
&+ \left(-2\ell_m^2 - 12\ell_m + \frac{8}{3}\ln 2 + \frac{\pi^2}{3} + \frac{160}{3}\right)L_M^2\\
&+ \left(-8\ell_m^2 + \left(\frac{16}{3}\ln 2 + \frac{2}{3}\pi^2 + \frac{320}{3}\right)\ell_m\right.\\
&- \; 288\ln 2 + \frac{4}{3}\pi^2 + 32\Big)L_M\\
&+ 56\ell_m^2 + \left(-288\ln 2 + \frac{4}{3}\pi^2 + 32\right)\ell_m\\
&+ \frac{3088}{9}\ln^2 2 - \frac{800}{9}\ln 2\\
&\left.\left. - \; \frac{\pi^4}{18} - \frac{8}{9}\pi^2\ln 2 - \frac{14}{3}\pi^2 + \frac{16}{9}\right]\cos^2\theta\right\}\beta^2 + \mathcal{O}(\beta^3),
\end{aligned}
$$

with

$$
L_M \equiv \ln\frac{4M^2}{m^2} \quad \text{and} \quad \ell_m \equiv \ln\frac{m^2}{\lambda^2}. \qquad (17)
$$

Hence we conclude that the result in (16), proportional to $\alpha^4\beta^2$, represents a N^{4}LO correction with respect to the LO result (the tree-level $e^+e^-\to f\bar f$ amplitude squared, which is already of $\mathcal{O}(\alpha^2)$). In [7], box amplitudes were not included with the rest of the one-loop diagrams to complete the NNLO calculation of $\sigma(e^+e^-\to\tau^+\tau^-)$ at threshold, their behavior with β being unknown. Our evaluation of $|\mathcal{M}_{\rm box}|^2$ has proven that this is, indeed, β^2 suppressed with respect the NNLO contributions considered in [7].

4 Threshold amplitude by asymptotic expansion of integrals

The counting of powers of the velocity appearing in a defined amplitude is not straightforward because β is not a parameter in the Lagrangian, but rather a dynamic scale which is driven by the propagators inside loop integrals. In recent years, this issue made it awkward to define a non-relativistic effective theory suitable for describing quarks and leptons at low velocities. Important progress was made after the development of the threshold expansion by Beneke and Smirnov [10]. This technique allows for an asymptotic expansion of Feynman integrals near threshold, providing a set of much simpler integrals which are manifestly homogeneous in the expansion parameter and so have a definite power counting in the velocity. The procedure should confirm that the two-photon box amplitude is not enhanced at low β, as we have found by explicit evaluation. This we discuss in the following.

The expansion method, described in [10], begins by identifying the relevant momentum regions in the loop integrals, which follow from the singularity structure of the Feynman propagators dictated by the relevant scales that appear in the problem. For on-shell scattering amplitudes of heavy fermions, three scales are identified: the heavy fermions mass, M, their relative three-momentum, $|\boldsymbol{k}|\sim M\beta$ and their energy $k_0\sim M\beta^2$. Accordingly, the loop four-momentum near the singularities can be in any of the following regimes:

$$
\begin{aligned}
\text{hard}: &\quad \ell_0\sim|\boldsymbol{\ell}|\sim M,\\
\text{soft}: &\quad \ell_0\sim|\boldsymbol{\ell}|\sim M\beta,\\
\text{potential}: &\quad \ell_0\sim M\beta^2,\quad |\boldsymbol{\ell}|\sim M\beta,\\
\text{ultrasoft}: &\quad \ell_0\sim|\boldsymbol{\ell}|\sim M\beta^2. \qquad (18)
\end{aligned}
$$

The original integral is then decomposed into a set of integrals, one for every region, and a Taylor expansion in the parameters, which are small in each regime, is performed. Every integral, containing just one scale, will thus contribute only to a single power in the velocity expansion.

The procedure requires the use of dimensional regularization in handling the integrals, even if they are finite, in order to assure that the result from each regime just picks up the corresponding pole contribution and vanishes outside it. Following these heuristic rules, the authors of [10] reproduce the exact β expansion of some one-loop and two-loop examples. Although a formal proof of the validity of the asymptotic expansion close to threshold has not been given, the perfect agreement in the examples supports their use in general one-loop diagrams. We provide a new test by addressing the rules to the QED box amplitude with e^+e^- in the initial state, extending the use of the threshold expansion to diagrams with heavy and massless fermions in the external legs (i.e. production-like diagrams). We will keep the electron mass finite along the procedure, although much smaller than any other scale, to keep track of the logarithms of m present in the box amplitude.

Our amplitude $\mathcal{M}_{\rm box}$ is characterized, as shown in Appendix A, by the four-point integrals $D_0, D_\mu, D_{\mu\nu}$ in (A.1). If present, inverse powers of the velocity in $\mathcal{M}_{\rm box}$ can only originate from these integrals. In addition, we can focus on the behavior of the scalar integral D_0, as the $\ell_\mu, \ell_\mu\ell_\nu$ vectors in D_μ and $D_{\mu\nu}$ will produce factors of one of the scales of the problem ($M, M\beta$ or $M\beta^2$) in the numerator of the amplitude without affecting the leading singular behavior in β. Let us change the routing of momenta in D_0 (A.1) in order to make the scaling arguments more transparent:

$$D_0 = \int \frac{\mathrm{d}^D\ell}{\mathrm{i}(2\pi)^D} \left\{ \frac{1}{[(Q/2+T/2-\ell)^2-m^2]} \times \frac{1}{[(Q/2+R/2-\ell)^2-M^2][\ell^2-\lambda^2]} \times \frac{1}{[(Q-\ell)^2-\lambda^2]} \right\}, \tag{19}$$

where the standard $+\mathrm{i}\delta$ prescriptions are implicitly understood in the propagators, the Q and R vectors are defined in relation with (A.1) and $T = p - p'$. The external four-vectors Q and R scale as M and $M\beta$ respectively, while $T^2 = -s + 4m^2 \sim M^2$. Using momentum T is preferred to the electron (positron) momentum p (p') because the spatial and time components of the latter, although they scale as M, are canceled in the total momentum squared $p^2 = m^2 \sim 0$. The infrared regularization of the integrals is automatically guaranteed by dimensional regularization and, therefore, we will not longer retain a fictitious mass for the photon.

In the potential region $\ell_0 \ll |\boldsymbol{\ell}| \ll M$ and, accordingly, we can expand terms in the propagators. The leading contribution is

$$D_0^p = \int \frac{\mathrm{d}^D\ell}{\mathrm{i}(2\pi)^D} \frac{1}{(\boldsymbol{\ell}\cdot\boldsymbol{T})(-\boldsymbol{\ell}^2+\boldsymbol{\ell}\cdot\boldsymbol{R}-Q_0\ell_0)(-\boldsymbol{\ell}^2)(Q_0^2)}, \tag{20}$$

where we have also dropped the term $-\boldsymbol{\ell}^2$ in the electron propagator to be compared to $\boldsymbol{\ell}\cdot\boldsymbol{T} \sim M^2\beta$. The overall scaling of the potential integration is easily estimated to be of order $M^4\beta^5/M^8\beta^5 \sim 1/M^4$, so no velocity enhancement in this region is expected. In fact, the integral above is zero because, closing the ℓ_0 integration contour in the lower half-plane, the pole at $\ell_0 = (\boldsymbol{\ell}\cdot\boldsymbol{R}-\boldsymbol{\ell}^2)/Q_0 + \mathrm{i}\delta$ lies outside[3]. Similarly, subleading terms in the expansion of propagators in this region are vanishing, as they share the same pole structure.

When the loop momentum ℓ is soft or ultrasoft, the assumption $\ell_0 \sim |\boldsymbol{\ell}| \ll M$ leads to the same expansion of the propagators in D_0:

$$D_0^{s,us} = \int \frac{\mathrm{d}^D\ell}{\mathrm{i}(2\pi)^D} \frac{1}{(\boldsymbol{\ell}\cdot\boldsymbol{T}-Q_0\ell_0)(-Q_0\ell_0)(\ell_0^2-\boldsymbol{\ell}^2)(Q_0^2)}. \tag{21}$$

It scales as $1/M^4$ in both the soft and ultrasoft regimes and, indeed, vanishes in dimensional regularization because, after picking up the residue in the lower plane, $\ell_0 = |\boldsymbol{\ell}| - \mathrm{i}\delta$, the remaining $D-1$ dimension integral is scaleless:

$$\begin{aligned} D_0^{s,us} &= \frac{1}{2Q_0^3}\int \frac{\mathrm{d}^{D-1}\ell}{(2\pi)^{D-1}} \frac{1}{|\boldsymbol{\ell}|^2} \frac{1}{(Q_0|\boldsymbol{\ell}|-\boldsymbol{T}\cdot\boldsymbol{\ell})} \\ &= \frac{1}{2Q_0^3}\int \frac{\mathrm{d}\Omega_{D-1}}{(2\pi)^{D-1}} \frac{1}{(Q_0-|\boldsymbol{T}|\cos\varphi)} \\ &\quad \times \int \mathrm{d}|\boldsymbol{\ell}||\boldsymbol{\ell}|^{D-2}\frac{1}{|\boldsymbol{\ell}|^3} = 0, \end{aligned} \tag{22}$$

with φ the angle between the vectors $\boldsymbol{T}$ and $\boldsymbol{\ell}$. The same argument holds for subleading terms in this region.

Finally, the integral in the hard region is obtained by dropping out terms involving non-relativistic fermion three-momenta from propagators. Hence, the only scale which remains is the hard parameter M, so there is no additional velocity dependence in the denominators. More explicitly, the expanded integral in the hard regime, at leading order in β, is

$$D_0^{h,\mathcal{O}(1)} = \int \frac{\mathrm{d}^D\ell}{\mathrm{i}(2\pi)^D} \times \frac{1}{(\ell^2-\ell\cdot T-Q\cdot\ell)(\ell^2-Q\cdot\ell)\ell^2(Q-\ell)^2}, \tag{23}$$

and there is no need to separate time from spatial components in the integration. The above integral trivially scales a $1/M^4$, and its explicit calculation in $D = 4-2\epsilon$ dimensions has been performed following [11]:

$$D_0^{h,\mathcal{O}(1)} = \frac{\mu^{-2\epsilon}}{8\pi s^2}\ln\frac{s}{m^2} \times \left[\frac{1}{\epsilon} - \ln\left(\frac{-s-\mathrm{i}\delta}{\mu^2}\right) + \ln(4\pi) - \gamma_{\rm E}\right], \tag{24}$$

[3] Notice that the ℓ_0 integration in D_0^p does not vanish in the outer semicircle. Rigorously we should keep the ℓ_0^2 term in the heavy fermion propagator, so D_0^p is well defined. Poles would then be located at $\ell_0^\pm = (1/2)(Q_0 \pm (Q_0^2 - 4(\boldsymbol{\ell}\cdot\boldsymbol{R}-\boldsymbol{\ell}^2) - \mathrm{i}\delta)^{1/2})$. The root ℓ_0^+ scales as M and is taken into account in the hard region while $\ell_0^- = (\boldsymbol{\ell}\cdot\boldsymbol{R}-\boldsymbol{\ell}^2)/Q_0 + \mathrm{i}\delta$ once we consider that $|\boldsymbol{\ell}| \ll M$ in the potential region, and we recover the above result

where $\gamma_{\rm E}$ is the Euler–Mascheroni constant. Terms proportional to the electron mass m have been dropped. The pole in (24) is of infrared origin, and it is the analogous to the $\ln\lambda^2$ term in the full result of D_0, (A.5). Indeed, (24) reproduces the leading term in the velocity expansion of D_0, after the usual replacement $\ln\lambda^2 \to (4\pi)^\epsilon/\Gamma(1-\epsilon)/\epsilon$.

The following order in the expansion within the hard region would have a $\ell\cdot R = -\boldsymbol{\ell}\cdot\boldsymbol{R}$ term in the numerator, and it would behave as β/M^4:

$$\begin{aligned} &D_0^{h,\mathcal{O}(\beta)} \\ &= \int \frac{{\rm d}^D\ell}{{\rm i}(2\pi)^D} \frac{\ell\cdot R}{(\ell^2-\ell\cdot T-Q\cdot\ell)(\ell^2-Q\cdot\ell)^2\ell^2(Q-\ell)^2} \\ &= \frac{R\cdot T}{T^2}\left(D_0^h - \int \frac{{\rm d}^D\ell}{{\rm i}(2\pi)^D}\frac{1}{(\ell^2-Q\cdot\ell)^2\ell^2(Q-\ell)^2}\right) \\ &= \frac{\beta\cos\theta}{8\pi^2 s^2}\mu^{-2\epsilon}\left(\ln\frac{s}{m^2}-2\right) \\ &\times\left[\frac{1}{\epsilon} - \ln\left(\frac{-s-{\rm i}\delta}{\mu^2}\right) + \ln(4\pi) - \gamma_{\rm E}\right], \end{aligned} \tag{25}$$

which agrees with the second term in the velocity expansion of D_0. The series expansion in β of the scalar function D_0 is thus reproduced by that of D_0^h, while the rest of the integration regions does not contribute at all.

Therefore we have seen, by asymptotic expanding the integral before its computation, that the box amplitude receives no contributions from the regions of potential, soft and ultrasoft loop momentum, and it is then preserved from Coulomb type singularities, as was shown by explicit calculation. This fact reveals that, as expected, the box production graph is a process dominated by the high scale, as it involves annihilating photons which carry energies of the order of the mass of the non-relativistic fermions.

Let us finally note that, although we have reproduced the (logarithmic) electron mass dependence of D_0 through the threshold expansion technique, we could, a priori, need to consider new regions to successfully obtain the subleading terms $\mathcal{O}(m^2/M^2)$, $\mathcal{O}(m^2/(q^2-4M^2))$, etc. This is what happens, for example, if one considers the one-loop two-point scalar function with one heavy mass M and one light mass m at values of $q^2 \gtrsim M^2$: Keeping m finite but smaller than any other scale present (i.e. $m \ll (q^2-M^2)/M \ll (q^2-M^2)^{1/2} \ll M$), the integration region where $\ell^2 \sim m^2$ gives a non-vanishing contribution proportional to $m^2/(q^2-M^2)$. A new pattern of integration regimes should then be considered to make each integral homogeneous also in the m^2 scale.

5 Conclusions

The interest in the study of electron positron annihilation into heavy fermions has been ushered by the multiple features foreseen both in high-energy colliders and production at threshold. These include all-important aspects of the phenomenology like an accurate measurement of the heavy fermion masses (like τ or t) and, the possibility, of exploring new physics beyond the standard model. This goal requires the computation and implementation of complete perturbative orders within the standard model.

We have evaluated the QED two-photon box diagrams of Fig. 1 contributing to $\sigma(e^+e^-\to f\bar f)$ with massive final fermions ($m_e \ll M$), and we have provided a full analytical expression for the amplitude. Its contribution at the production threshold has also been studied and we have found that it is negligible because of the high velocity suppression. This non-relativistic analysis complements the one carried out in [7] and shows that the conclusions reached in that reference are not modified by the QED box amplitude.

Finally we have analyzed this low velocity behavior using the strategy of regions to expand the Feynman integrals near threshold, confirming that such an expansion can also be applied to diagrams involving heavy and light fermions. This feature allows one to identify and evaluate, at a fixed order in the heavy fermion velocity, contributions to heavy fermion production or annihilation diagrams triggered by light fermions.

Acknowledgements. We wish to thank A. Pich for relevant discussions on the subject of this paper and for a careful reading of the manuscript. The work of P.D. Ruiz-Femenía has been partially supported by a FPU scholarship of the Spanish Ministerio de Educación y Cultura. J. Portolés is supported by a "Ramón y Cajal" contract with CSIC funded by MCYT. This work has been supported in part by TMR, EC Contract No. ERB FMRX-CT98-0169, by MCYT (Spain) under grant FPA2001-3031, and by ERDF funds from the European Commission.

Appendix

A Integrals in the box amplitude

In this appendix we outline several features of the integration procedure, in order to evaluate the QED box diagrams, and we collect the explicit expressions for the relevant scalar integrals that appear in our results.

The general structure of the two-photon box amplitude in Fig. 1a, $\mathcal{M}_a$ takes the form $\mathcal{M}_a = a_0 D_0 + a^\mu D_\mu + a^{\mu\nu}D_{\mu\nu}$, where $a_0, a_\mu, a_{\mu\nu}$ contain Dirac algebra γ's and spinors, and $D_0, D_\mu, D_{\mu\nu}$ are the integrals over the loop momentum ℓ:

$$\begin{aligned} D_0; D_\mu; D_{\mu\nu} = \int \frac{{\rm d}^4\ell}{{\rm i}(2\pi)^4}\frac{1;\ell_\mu;\ell_\mu\ell_\nu}{(\ell^2-m^2)} \\ \times\frac{1}{[(\ell+k-p)^2-M^2][(\ell-p)^2-\lambda^2][(\ell+p')^2-\lambda^2]}, \end{aligned} \tag{A.1}$$

which depend on three independent four-vectors and where $+{\rm i}\delta$ prescriptions are understood in the propagators. Let us define our basis as $P = p-k, Q = p+p'$ and $R = k-k'$, with scalar products

$$P^2 = t, \quad Q^2 = s, \quad R^2 = 4M^2 - s,$$

$$P\cdot Q = 0, \quad P\cdot R = m^2 - M^2 - t, \quad Q\cdot R = 0.$$

The integrals in (A.1) are invariant under the interchange $\{p;k\} \leftrightarrow \{-p';-k'\}$. Under the same transformation $P \to P$, $Q \to -Q$ and $R \to R$, and thus the tensor integrals $D_\mu, D_{\mu\nu}$ do not contain terms linear in Q, justifying our choice of basis. The tensor decomposition of $D_\mu, D_{\mu\nu}$ then reads

$$D_\mu = D_P P_\mu + D_R R_\mu \tag{A.2}$$

$$D_{\mu\nu} = D_{PP} P_\mu P_\nu + D_{PR}(P_\mu R_\nu + R_\mu P_\nu) + D_{RR} R_\mu R_\nu + D_{QQ} Q_\mu Q_\nu + s D_{00} g_{\mu\nu}. \tag{A.3}$$

Further reduction of the coefficient functions appearing in (A.2) and (A.3) has been performed with the help of FeynCalc [12]. These coefficients are thus expressed as a linear combination of a set of scalar integrals: D_0, C_s, C_t, C_M, B_s, B_t and B_M, with the four (D_0), three (C_a, $a = s,t,M$) and two (B_a, $a = s,t$) propagators that we collect next.

The relevant scalar integrals have been evaluated following the method described in [13], except for the rather cumbersome four-point function D_0. In the latter case we have first calculated its imaginary part in the s-channel, in accordance with the optical theorem, and then the real part has been reconstructed through the t-fixed unsubtracted dispersion relation that satisfies D_0:

$$\mathrm{Re}D_0(s,t) = \frac{1}{\pi} \fint_{4\lambda^2}^{\infty} \mathrm{d}x \frac{\mathrm{Im}D_0(x,t)}{x-s}, \tag{A.4}$$

where the Principal Value of the integral is understood. We have performed its calculation in the $\lambda \ll m \ll M$ limit and, therefore, we have neglected photon masses when possible. As emphasized in [14], the limit $\lambda \to 0$ is not trivial for the occurrence of terms like $\lambda^2/(x-4\lambda^2)$, which diverge for finite λ as $x \to 4\lambda^2$ but vanish for $\lambda \to 0$ at fixed $x \neq 4\lambda^2$. As a consequence the photon mass should be kept finite until the final stages.

The scalar integrals that appear in the two-photon box amplitude result in (3) through the $\mathcal{F}_i$ functions of (7)–(10) have been evaluated in the limit where $\lambda \ll m \ll M$ and for the specific cases $p^2 = p'^2 = m^2$, $k^2 = k'^2 = M^2$, $(p+p')^2 = (k+k')^2 = s$, $(p-k)^2 = t$. They read

$$\begin{aligned} D_0 &= \int \frac{\mathrm{d}^4\ell}{\mathrm{i}(2\pi)^4} \frac{1}{[\ell^2-\lambda^2][(\ell+p)^2-m^2)]} \\ &\times \frac{1}{[(\ell+p+p')^2-\lambda^2][(\ell+k)^2-M^2]} \\ &= \frac{-1}{8\pi^2 s(M^2-t)} \ln\frac{M^2-t}{mM} \ln\frac{-s-\mathrm{i}\delta}{\lambda^2}, \end{aligned} \tag{A.5}$$

$$\overline{D}_0 = D_0(t \to u), \tag{A.6}$$

$$\begin{aligned} C_s &= \int \frac{\mathrm{d}^4\ell}{\mathrm{i}(2\pi)^4} \\ &\times \frac{1}{[\ell^2-\lambda^2][(\ell+p)^2-m^2][(\ell+p+p')^2-\lambda^2]} \\ &= \frac{1}{32\pi^2 s}\left[\ln^2\left(\frac{-s-\mathrm{i}\delta}{m^2}\right) + \frac{\pi^2}{3}\right], \end{aligned} \tag{A.7}$$

$$\begin{aligned} C_t &= \int \frac{\mathrm{d}^4\ell}{\mathrm{i}(2\pi)^4} \\ &\times \frac{1}{[\ell^2-M^2][(\ell-k)^2-\lambda^2][(\ell+p-k)^2-m^2]} \\ &= \frac{-1}{16\pi^2(M^2-t)}\left[\mathrm{Li}_2\left(\frac{t}{M^2}\right) + \ln^2\left(\frac{M^2-t}{Mm}\right)\right. \\ &\left. + \ln\left(\frac{M^2-t}{Mm}\right)\ln\left(\frac{m^2}{\lambda^2}\right)\right], \end{aligned} \tag{A.8}$$

$$\overline{C}_t = C_t(t \to u), \tag{A.9}$$

$$\begin{aligned} C_M &= \int \frac{\mathrm{d}^4\ell}{\mathrm{i}(2\pi)^4} \\ &\times \frac{1}{[\ell^2-\lambda^2][(\ell+k)^2-M^2][(\ell+k+k')^2-\lambda^2]} \\ &= \frac{1}{16\pi^2 s\beta}\left[-2\mathrm{Li}_2(1-\beta) + 2\mathrm{Li}_2\left(\frac{1-\beta}{1+\beta}\right)\right. \\ &+ \frac{1}{2}\ln^2\left(\frac{1-\beta}{1+\beta}\right) - 2\mathrm{Li}_2(-\beta) \\ &\left. - 2\ln\beta\ln(1+\beta) + \mathrm{i}\pi\ln\frac{1-\beta}{1+\beta}\right], \end{aligned} \tag{A.10}$$

$$\begin{aligned} B_s &= \int \frac{\mathrm{d}^D\ell}{\mathrm{i}(2\pi)^D} \frac{1}{[\ell^2-\lambda^2][(\ell+p+p')^2-\lambda^2]} \\ &= \frac{-1}{16\pi^2}\left(\Delta + \ln\frac{-s-\mathrm{i}\delta}{\mu^2} - 2\right), \end{aligned} \tag{A.11}$$

$$\begin{aligned} B_t &= \int \frac{\mathrm{d}^D\ell}{\mathrm{i}(2\pi)^D} \frac{1}{[\ell^2-M^2][(\ell+p-k)^2-m^2]} \\ &= \frac{-1}{16\pi^2}\left(\Delta + \ln\frac{-t}{\mu^2} + \ln\left(1-\frac{M^2}{t}\right)\right. \\ &\left. - \frac{M^2}{t}\ln\frac{M^2-t}{M^2} - 2\right), \end{aligned} \tag{A.12}$$

$$\begin{aligned} B_M &= \int \frac{\mathrm{d}^D\ell}{\mathrm{i}(2\pi)^D} \frac{1}{[\ell^2-\lambda^2][(\ell+k)^2-M^2]} \\ &= \frac{-1}{16\pi^2}\left(\Delta + \ln\frac{M^2}{\mu^2} - 2\right), \end{aligned} \tag{A.13}$$

where $\mathrm{Li}_2(x)$ is the dilogarithm function. The two-point functions have been regularized within dimensional regularization in D dimensions and $\Delta = 2\mu^{D-4}/(D-4) + \gamma_\mathrm{E} - \ln(4\pi)$, with μ the renormalization scale. From the full expressions above we see that only the integrals C_t, $\overline{C}_t$, D_0 and $\overline{D}_0$ are infrared divergent for vanishing photon mass ($\lambda \to 0$). However, as remarked in the main text, the combinations sD_0–$2C_t$ (or $s\overline{D}_0$–$2\overline{C}_t$) are infrared finite; accordingly all the infrared divergent contribution is provided by D_0 and $\overline{D}_0$ in (11) that carry a $\ln\lambda^2$ factor.

B Infrared divergence of the QED box diagram

There are several well-known facts on the structure of infrared divergences in QED that are relevant for our discussion [15]:

(1) Virtual photon radiative corrections between the external legs of a divergenceless root diagram generate

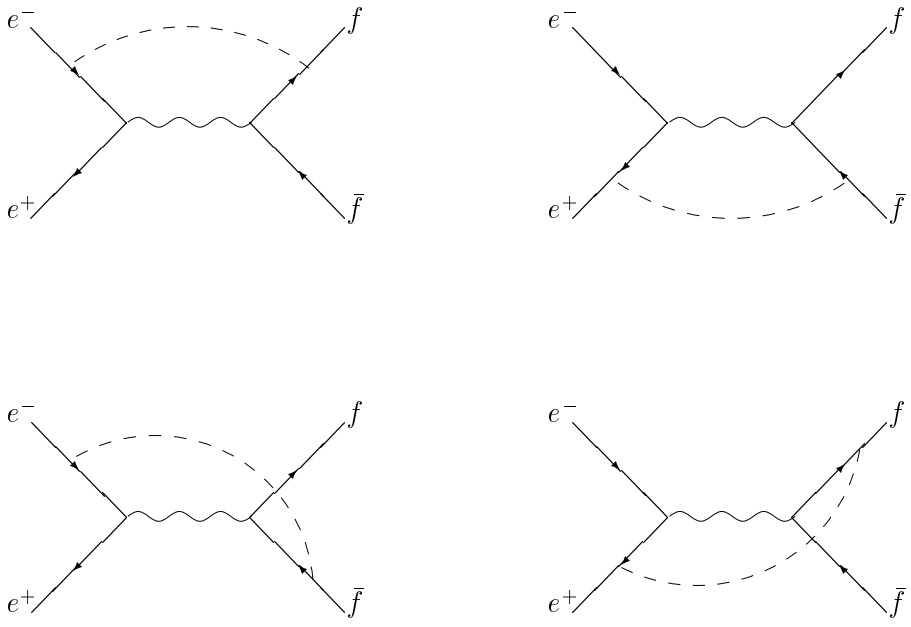

Fig. 2. Diagrams contributing to the infrared divergence of the QED box diagram. The wavy line corresponds to a hard photon and the dashed line to a soft photon. As explained in the text the infrared divergence factorizes and the spinor structure is the one of the hard diagram (without radiative corrections)

an infrared divergent contribution that follows a specific pattern in the perturbative expansion. Such a structure provides a factorization of the resummation of the divergences at all orders.

(2) The whole infrared divergence in virtual photon radiative corrections commented on above arises from the eikonal approach in the propagator of the radiating external legs. For spin 1/2, for example, with k the outgoing soft photon momentum of $\varepsilon_\mu(k)$ polarization and p the ingoing external momentum, the modification of the fermion wave function reads

$$u(p) \xrightarrow{\text{photon}} \frac{1}{\not{p} - \not{k} - m + \mathrm{i}\delta} \not{\varepsilon} u(p) = \frac{(2p-k)\cdot\varepsilon - \frac{1}{2}[\not{k}, \not{\varepsilon}]}{k^2 - 2k\cdot p + \mathrm{i}\delta} u(p), \qquad \text{(B.1)}$$

which in the eikonal approximation reduces to

$$u(p) \xrightarrow[\text{photon}]{\text{soft}} \frac{2p\cdot\varepsilon}{k^2 - 2k\cdot p + \mathrm{i}\delta} u(p), \qquad \text{(B.2)}$$

neglecting, essentially, the spin of the radiating field.

Hence to extract the infrared divergent part of the QED box diagram in Fig. 1 we need to implement the eikonal approximation into the amplitude $\mathcal{M}_a$ in (2) and the crossed $\mathcal{M}_b$. This corresponds to the evaluation of the four diagrams in Fig. 2. These are built from the tree-level diagram for $e^+e^- \to f\bar{f}$ through one-photon annihilation, by attaching a soft photon between an ingoing and an outgoing external leg in all possible ways. Their evaluation gives

$$\mathcal{M}_{\text{box}}^{\text{IR}} = \overline{v}_e(p')\gamma_\mu u_e(p) \frac{e^2 Q_f}{s} \overline{u}_f(k)\gamma^\mu v_f(k') \times \left[\frac{e^2 Q_f}{4\pi^2} \ln\left(\frac{M^2-u}{M^2-t}\right) \ln\left(\frac{m^2}{\lambda^2}\right)\right], \qquad \text{(B.3)}$$

where infrared finite terms have not been written. In fact, this result has been obtained by integrating over the full range of momentum of a massive photon. Rigorously we should define the infrared contribution by imposing an upper limit on its momentum $|\boldsymbol{q}_\gamma| < \Lambda$, and m^2 would then be replaced by Λ^2 in the logarithm of $\mathcal{M}_{\text{box}}^{\text{IR}}$. In (B.3) we have explicitly stated the factorization between the hard gluon exchange, on the left, and the soft photon exchange inside the square brackets.

Alternatively we can evaluate $\mathcal{M}_{\text{box}}^{\text{IR}}$ from our result in (3) and we obtain

$$\mathcal{M}_{\text{box}}^{\text{IR}} = \frac{e^4 Q_f^2}{8\pi^2 s} \times \left\{ \frac{(M^2-t)L_1^{-\kappa} + 2L_2^{+\kappa} - M\left(L_4^{+\kappa} - L_4^{-\kappa}\right)}{M^2-t} \ln\left(\frac{M^2-t}{Mm}\right) - \frac{(M^2-u)L_1^{+\kappa} - 2L_2^{-\kappa} - M\left(L_4^{+\kappa} - L_4^{-\kappa}\right)}{M^2-u} \ln\left(\frac{M^2-u}{Mm}\right) \right\} \times \ln\left(\frac{\lambda^2}{-s-\mathrm{i}\delta}\right), \qquad \text{(B.4)}$$

where the spinor operators $L_i^{\rho\kappa}$ have been defined in (4). Then, using the following relations[4]:

$$(M^2-t)L_1^{+\kappa} = 2L_2^{+\kappa} - M\left(L_4^{+\kappa} - L_4^{-\kappa}\right), \quad (M^2-u)L_1^{-\kappa} = -2L_2^{-\kappa} - M\left(L_4^{+\kappa} - L_4^{-\kappa}\right), \qquad \text{(B.5)}$$

we finally get

$$\mathcal{M}_{\text{box}}^{\text{IR}} = \frac{e^2 Q_f}{2s}\left(L_1^{+\kappa} + L_1^{-\kappa}\right)$$

[4] Relations between spinor operators like these can be obtained by explicit evaluation in a particular reference frame or transforming the operators into traces in the spinor basis, hence working with Lorentz invariant expressions

$$\times \left[\frac{e^2 Q_f}{4\pi^2} \ln\left(\frac{M^2-u}{M^2-t}\right) \ln\left(\frac{-s-\mathrm{i}\delta}{\lambda^2}\right)\right], \quad \text{(B.6)}$$

whose infrared logarithm coincides with our previous result in (B.3), since $P_\kappa u_e(p) = u_e(p)$ in $L_1^{\pm\kappa}$, κ being the massless electron helicity.

We conclude that the infrared divergence of the QED box diagram satisfies the expected features [15] and hence its cancellation should take place when real soft photon radiation contributions, at a fixed α perturbative order, are taken into account.

References

1. D.Y. Bardin, P. Christova, M. Jack, L. Kalinovskaya, A. Olchevski, S. Riemann, T. Riemann, Comput. Phys. Commun. **133**, 229 (2001) [hep-ph/9908433]
2. D.Y. Bardin, L. Kalinovskaya, G. Nanava, An electroweak library for the calculation of EWRC to e+ e- → f anti-f within the topfit project, hep-ph/0012080
3. A. Andonov, D. Bardin, S. Bondarenko, P. Christova, L. Kalinovskaya, G. Nanava, Further study of the $e + e- \to f\mathrm{anti} - f$ process with the aid of CalcPHEP system, hep-ph/0202112
4. R. Barbieri, P. Christillin, E. Remiddi, Phys. Rev. A **8**, 2266 (1973)
5. W.E. Caswell, G.P. Lepage, Phys. Lett. B **167**, 437 (1986); A. Pineda, J. Soto, Nucl. Phys. Proc. Suppl. **64**, 428 (1998) [hep-ph/9707481]; M.E. Luke, A.V. Manohar, I.Z. Rothstein, Phys. Rev. D **61**, 074025 (2000) [hep-ph/9910209]
6. J.M. Jowett, Initial Design Of The Cern Tau Charm Factory, CERN-LEP-TH/87-56; A. Pich, Perspectives on tau charm factory physics, hep-ph/9312270
7. P. Ruiz-Femenia, A. Pich, Phys. Rev. D **64**, 053001 (2001) [hep-ph/0103259]
8. A.H. Hoang, A.V. Manohar, I.W. Stewart, T. Teubner, Phys. Rev. Lett. **86**, 1951 (2001) [hep-ph/0011254]
9. W. Beenakker, S.C. van der Marck, W. Hollik, Nucl. Phys. B **365**, 24 (1991)
10. M. Beneke, V.A. Smirnov, Nucl. Phys. B **522**, 321 (1998) [hep-ph/9711391]
11. Z. Bern, L.J. Dixon, D.A. Kosower, Phys. Lett. B **302**, 299 (1993) [Erratum ibid. B **318**, 649 (1993)] [hep-ph/9212308]
12. R. Mertig, M. Bohm, A. Denner, Comput. Phys. Commun. **64**, 345 (1991), http://www.feyncalc.org
13. G. 't Hooft, M. Veltman, Nucl. Phys. B **153**, 365 (1979)
14. R. Barbieri, J.A. Mignaco, E. Remiddi, Nuovo Cim. A **11**, 824 (1972)
15. D.R. Yennie, S.C. Frautschi, H. Suura, Annals Phys. **13**, 379 (1961); N. Meister, D.R. Yennie, Phys. Rev. **130**, 1210 (1963); S. Weinberg, Phys. Rev. B **140**, 516 (1965)